Monitoring Stratospheric OClO with Sentinel-5p (S5pOClO)

Sentinel-5p + Innovation - Theme 2: Chlorine Dioxide

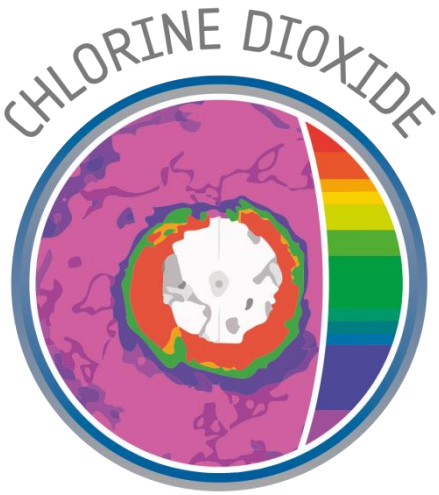

Validation Report

document number	:	S5p+I_OCLO_BIRA_VR
authors	:	Gaia Pinardi, Andreas Richter, Andreas Meier, Michel Van Roozendael
issue	:	2.0
date	:	2023-08-15
status	:	Final
Data contributors	:	Myojeong Gu, Thomas Wagner, Kristof Bognar, Ramina Alwarda, Kimberly Strong, Udo Friess, Richard Querel, Cristina Prados-Roman, Margarita Yela Gonzalez

Contents

1 Purpose and objective

The purpose of this Validation Report (VR) is to describe the validation performed on the S5p+I Level-2 OClO product. It contains a review of collected OClO ground-based datasets, the OClO SCD comparison methods, and a summary of validation results.

This document will be maintained during the development phase and the lifetime of the data products. Updates and new versions will be issued in case of changes in the processing chains or for novel validation exercises. The current validation report version (v2.0) is thus an update of report v1.1, replacing previous S5p OClO dataset v0.9 with current version v0.97 and extending the validation results to April 2021 with updated ground-based datasets (and sometimes revisited, as for IUPH).

2 Document overview

Section 4 gives a summary of the requirements on OClO retrievals, Section 5 presents shortly the S5p OClO dataset v0.97 validated here and Section 6 introduces the ground-based data used for this validation report. Section 7 contains a description of the validation approach and Section 8 presents the results, as a function of different estimators. Sections 9, 10, and 11 present verification with other satellite data from OMI, GOME-2A and S5p, respectively.

3 References, terms and acronyms

3.1 References

[AD1] Sentinel-5p Innovation (S5p+I) - Statement of Work - EOP-SD-SOW-2018-049.
Source: ESA, **issue:** 2, date: 20/08/2018.

[AD2] Copernicus Sentinels 4 And 5 Mission Requirements Traceability Document, EOP-SM/2413/BV-bv.
Source: ESA, **issue:** 2.0, **date:** 07/07/2017.

[AD3] Sentinel-5 Level-2 Prototype Processor Development Requirements Specification, ESA, S5-RS-ESA-GR-0131.
Source: ESA, **issue:** 1.7, **date:** 29/06/2018.

[AD4] Sentinel-5p+Innovation: Theme 2; Monitoring Stratospheric OClO with Sentinel-5p (S5pOClO): Algorithm Theoretical Baseline Document.
Source: IUP-UB, **issue:** 3.0, **ref:** S5p+I_OCLO_IUP-UB_ATBD, **date:** 15/08/2023.

3.2 Terms, definitions and abbreviated terms

ATBD	Algorithm Theoretical Base Document
AC SAF	Atmospheric Composition Monitoring Satellite Application Facility
CTM	Chemistry Transport Model
DOAS	Differential Optical Absorption Spectroscopy

ESA	European Space Agency
GB	Ground-based
GOME-2A	Global Ozone Monitoring Experiment on MetOp-A
IASB-BIRA	Belgian Institute for Space Aeronomy
IUP-UB	Institute of Environmental Physics (Institut für Umweltphysik), University of Bremen
MPIC	Max Planck Institute for Chemistry
OMI	Ozone Monitoring Instrument
RTM	Radiative Transfer Model
SZA	Solar Zenith Angle
S-4, -5, -5P	Sentinel-4, -5, -5-Precursor
TROPOMI	TROPOspheric Monitoring Instrument
VR	Validation Report

4 Product requirements

S5p OClO scientific product requirements are mostly determined by the need to monitor stratospheric chlorine activation over time in order to document the continuing effectiveness of the measures taken in the Montreal Protocol and its amendments. Recent reports of unexpected emissions of CFCs (Rigby et al., 2019) underline the relevance of such monitoring. While OClO observations do not provide a direct measure of stratospheric chlorine concentrations, they are an indicator of stratospheric chlorine activation.

For long-term stratospheric monitoring, the most important aspect of the OClO data set is its internal consistency in order to draw reliable conclusions on atmospheric changes. For scientific applications outside of polar stratospheric ozone research such as detection of OClO in lee waves or volcanic emissions, the scientific requirements are mainly the avoidance of false positive detection in the presence of aerosols, clouds and temperature changes and a low noise.

To the knowledge of the authors, no operational thresholds or relative uncertainty requirements have been defined for OClO slant columns for any S5p/S5/S4 instrument so far. For the AC SAF OClO GOME2 product, there were general requirements: Threshold accuracy: 100%; Target accuracy: 50%; Optimal accuracy: 30%. Typical OClO slant columns observed at 90° SZA in the fully activated vortex are of the order of $2x10^{14}$ molec/cm^2. For GOME2, standard deviations of $6x10^{13}$ molec/cm^2 are found for individual measurements and systematic differences between the different GOME instruments of the order of 1-2x 10^{13} molec/cm^2 (Richter et al., 2015).

The requirements for ground-based datasets are related to their polar location, for the OClO sampling, and their quality. Quality assurance of the ground-based datasets involves the reporting of the error and a common verification for possible offsets (see Sect. 6.1.1).

5 S5p OClO data

The current document focuses on the validation of TROPOMI OClO v0.97, which is briefly summarized in the following Table 5.1. Three years of data have been analysed and provided for the validation. An illustration of the OClO values over the 4/2018 to 4/2021 period is given in Figure 5.1.

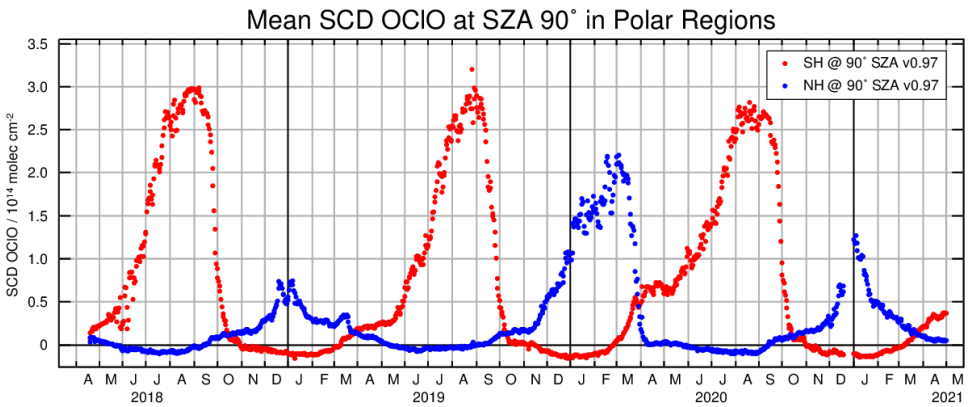

Figure 5.1: Time-series of daily TROPOMI mean OClO SCD around 90° SZA over Polar regions, separated by Southern Hemisphere (red) and Northern Hemisphere (blue).

Table 5.1: Description of the TROPOMI OClO datasets used in this study.

Analysis details	TROPOMI OClO v0.97	
Analysis window	345-389nm	
Cross-sections		
OClO	213 K	Kromminga et al., 2003
NO_2	220 K	Vandaele et at., 2002
O_4	293K	Thalman & Volkamer, 2013
O_3	223 K	Serdyuchenko et al., 2014
	243 K	Serdyuchenko et al., 2014
BrO (from separate fit in 334.6-358.0 nm window)	228 K	Wilmouth et al., 1999
Ring		Vountas et al., 1998
Mean fit residual northern hemisphere		Derived from single orbit orbit: 906220810 latitude: 60° -- 90° longitude: -180° -- 180°
Mean fit residual tropical Pacific		Derived from single orbit, orbit: 902012216 latitude: -10° -- -30° longitude: 200° -- 270°
Two cross-sections to correct for scene inhomogeneity effects		Derived from single orbit, orbit: 902012216
Polynomial	5. Order (6 coeffs.)	
Additive polynomial	offset and slope	
Background spectrum	Daily irradiance	
Post-processing	Destriping, offset correction	

The three-year time series starts in April 2018 with the continuous availability of S5p spectra. The time span until April 2021 covers the activation period 3 times in both hemispheres. A similar magnitude and duration of the activation period is observed for all southern hemispheric winters, as it is expected due to the usually stable southern polar vortex. For the northern hemisphere, the polar vortex is not as stable and chlorine dioxide levels which depend on the degree of chlorine activation on PSCs forming in the cold vortex area are more variable. The highest values are found in early 2020.

For the current version 0.97 of the S5p Prototype Product, a precision (1σ) of about $2\text{x}10^{13}$ molec/cm^2 is estimated from the scatter in the equatorial Pacific that increases to about $15\text{x}10^{13}$ molec/cm^2 at 90° SZA following largely the reduction of intensity and the increase in photon shot noise, see ATBD [AD3].

6 Reference measurements

In this VR, comparisons with ground-based data and satellite products are included. While comparison with satellite data can be considered as verification as they are very similar to the S5p OClO product, comparison to ground-based zenith-sky observations is seen as validation in spite of the fact that the spectral retrieval is similar for both instrument types.

6.1 Ground based monitoring network

OClO columns have been retrieved from the ground since 1986 using Differential Optical Absorption Spectroscopy (DOAS) measurements in the Antarctic and Arctic (Solomon et al., 1987; 1988; Kreher et

al., 1996; Gil et al., 1996; Richter et al., 1999; Tørnkvist et al., 2002; Vandaele et al., 2005; Friess et al., 2005).

Several zenith-sky DOAS instruments operating in the NDACC (https://www.ndaccdemo.org/) framework produce OClO slant columns, albeit usually not as their primary product. These data sets are available from the instrument operators. For this study, stations situated at latitudes above 60° (north and south) have been selected and OClO SCD data retrieved from different groups have been collected and used for validation of S5p OClO columns. An overview on the data available is given below and in Table 6.1.

Arctic:

- UToronto operates the PEARL UV-VIS spectrometer in Eureka (Nunavut, northern Canada). OClO SCD data have been analysed with a daily reference since 2007, and with a fixed annual reference since 2018.
- IUP-Bremen operates a UV-VIS spectrometer in Ny-Ålesund (Spitsbergen) since 1995 (Wittrock et al., 2004). OClO SCDs have been analysed since 2007 using one fixed reference for each season.
- MPIC operates a UV-VIS spectrometer in Kiruna (Sweden) since 1996. OClO SCDs have been analysed since 2007, with a special focus on the 2018-2020 period for the TROPOMI validation.
- BIRA-IASB operates a UV-VIS spectrometer in Harestua (Norway) since the ’90. End of 2012 a new instrument has been installed with an improved signal to noise ratio, and OClO SCDs have been analysed since then using annual reference spectra.

Antarctic:

- IUP-Heidelberg operates a UV-VIS spectrometer in the German research station of Neumayer (the ice shelf in the Atlantic sector of the Antarctic continent) since the ’90 (Friess et al., 2005). Generally, enhanced OClO signals are observed between August and October, when the polar vortex is over the station.
- IUP-Heidelberg operates a UV-VIS spectrometer in Arrival Heights (78°S, 167°E), part of the New Zealand station Scott Base on Ross Island since the ‘90 (Friess et al., 2005). Another instrument was present at the station, operated by NIWA (Kreher et al., 1996), but stopped measurements in 2017.
- INTA operates a UV-VIS spectrometer in the Belgrano II station, the Argentinian station situated on the coast of the Antarctic continent in the Weddell Sea area. Belgrano is representative of an in-polar vortex station during winter-spring season until the vortex breakdown (Yela et al., 2005, Puentedura et al. 2014). The UV instrument is measuring since February 2011 and OClO SCD have been analysed by INTA for 2011, 2015, 2016, 2018, 2019 and 2020.
- INTA operates a UV-VIS spectrometer at the Argentinian Marambio station, in Marambio Island (Graham Land, Antarctic Peninsula) since 2015. Marambio is frequently located in the vortex edge region and affected by both vortex air masses and mid-latitude air masses.

It can be seen in Figure 6.1 that this dataset ensures a good temporal coverage, with the different stations measuring at least one year in overlap with the S5p dataset (April 2018 to April 2021). A good coverage of the Arctic and Antarctic regions is also assured, with half of the stations in the Northern Hemisphere and half in the Southern Hemisphere. However, as briefly described in Table 6.2, the ensemble of ground-based datasets is an aggregate of existing measurements and there is no harmonization in the retrieval choices of the different groups processing the OClO data. Different wavelength regions for the OClO analysis have been used by each group, depending on their instrument's wavelength coverage and their sensitivity. The statistical error in OClO SCDs during twilight is on the order of 2 x10^{13} molec/cm² (Friess et al., 2005) for Neumayer and Arrival Heights. Random SCD errors are estimated by each group in their DOAS analysis, and values for the different datasets range from 6 to 22% for an SCD of about 1.5 x10^{14} molec/cm². Sensitivity tests have been performed to better characterize the impact of the different DOAS retrieval choices (OClO cross-sections, wavelength ranges, interfering species, the Ring effect, …) and to better assess the ground-based dataset consistency. Systematic uncertainties related to the OClO cross-section (Kromminga at al., 2003 at 213K with respect to other temperatures or with respect to the Wahner et al., 1987 choice) are e.g., on the order of 6% to -12% when tested on a few days of Ny-Ålesund OClO SCD analysis. Other systematic contributions related to the retrieval choices made here (see Table 6.2) have been estimated to be about 18%, leading to a total systematic uncertainty of about 25%. The total uncertainties vary thus between 22 and 31% for the different sites. More details can be found in Pinardi et al., 2022.

Table 6.1: Overview on ground-based data sets available

Location	Coordinates	Data Provider	Time Coverage
Eureka	80.05°N, 86.42°W	UToronto	2006-present
Ny-Ålesund	78.9°N, 11.9°E	IUPB	1995-present
Kiruna	67.9°N, 20.4°E	MPIC	1997-present
Harestua	60.22°N, 10.75°E	BIRA-IASB	1998-2013 2012-present
Marambio	64.3°S, 56.7°W	INTA	2015-present
Neumayer	70.62°S, 8.27°W	IUPH	2006-present
Arrival Heights	77.83°S, 166.65°W	IUPH NIWA	2006-present 2007-2017 (NIWA)
Belgrano	77.9°S, 34.6 °W	INTA	2011; 2015-present

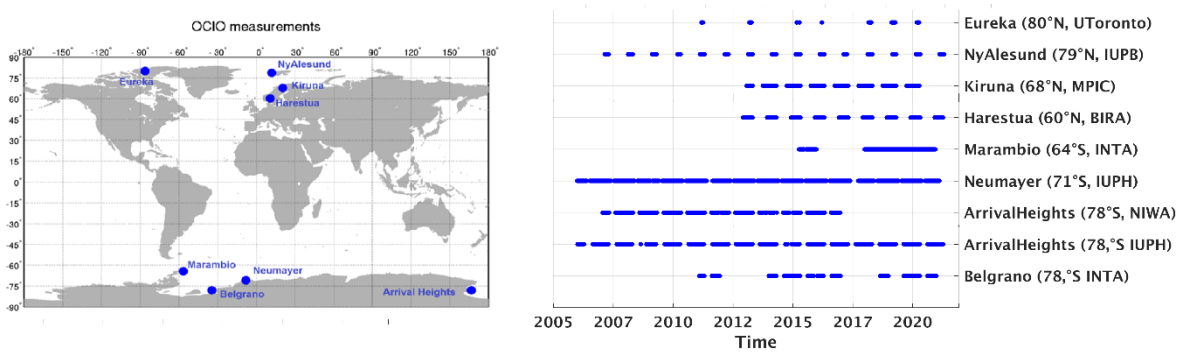

Figure 6.1: (left) Map and (right) time-lines of ground-based OClO SCD data collected for the TROPOMI validation.

Table 6.2: Description of the different ground-based OClO datasets used in this study, from Pinardi et al., 2022.

Group	Station	Coordinates	wavelength range (nm)	Cross-sections OClO	NO_2	O_3	BrO	O_4	Others
UToronto	Eureka	80.05°N, 86.42°W	350-380	[a] **(204K)**	[d] (220K)	[e] (223K)	[h] (223K)	[j] (296K)	Ring[n]
IUPB	Ny-Alesund	78.9°N, 11.9°E	365-388	[b] (213K)	[d] (220K)*	-	-	[l] (298K)	Ring[o]
MPIC	Kiruna	67.8°N, 20.4°E	372-392	[c] (213K), OClO×λ	[d] (220K)	[e] (223K)	-	[m] (273K)	Ring (213K, 263K) $Ring_1 \times \lambda^4$, $Ring_2 \times \lambda^4$
BIRA	Harestua	60.2°N, 10.7°E	347-374	[c] (213K)	[d] (220K)	[f] (223K, 243K)*	[h] (223K)	[m] (293K)	Ring[p]
INTA	Belgrano	77.9°S, 34.6°W	345-389	[c] **(233K)**	[d] (220K)*	[f] (223K,243K)*,+,	[h] (223K)	[m] (293K)	Ring[o] (250K)
	Marambio	64.3°S, 56.7°W							
IUPH	Neumayer	70.6°S, 8.3°W	364-391	[c] **(233K)**	[d] (220K, 298K)	[e] (223K, 293K)	[i] (228K)	[l] (298K)	Ring[n]
	Arrival Heights	77.8°S, 166.6°W							$Ring \times \lambda^4$
NIWA	Arrival Heights	77.8°S, 166.6°W	404-425	[c] (213K)	[d] (220K)	[g] (218K)	-	-	Ring and H_2O

[a] Wahner et al. (1987); [b] Kromminga et al. (1999); [c] Kromminga et al. (2003); [d] Vandaele et al. (1998); [e] Bogumil et al. (2003); [f] Serdyuchenko et al. (2014); [g] Brion et al. (1998); [h] Fleischmann et al. (2004); [i] Wilmouth et al. (1999); [j] Greenblatt et al. (1990); [k] Hermans et al. (2003); [l] Hermans et al. (1999); [m] Thalman and Volkamer (2013); [n] Chance and Spurr (1997); [o] QDOAS high resolution based on SAO: Chance and Kurucz (2010); [p] SCIATRAN
*: I0 correction (Aliwell et al. 2002); +: with Pukite et al. (2010) approach

Limitations:

- due to the limited number of stations, spatial coverage is poor and depending on the shape of the Polar Vortex, sampling biases can occur
- ensemble of different non-harmonized analysis, with different DOAS settings (see Table 6.2)
- sensitivity to the choice of the reference spectra, that should be defined ad-hoc to not contain OClO (e.g., use a fixed yearly reference outside the activation period), otherwise it could lead to offsets in the ground-based OClO SCD.

To overcome some of these limitations, interactions with the ground-based data providers are important, and lead to revision of some of the datasets with respect to previous versions of this report (extension in time and e.g. revision of Neumayer IUPH data). Moreover, a post-processing of the ground-based data has also been set-up at BIRA, to try to further homogenize the data and reduce possible biases, as described in the next sub-section and used in Sect. 8.1.2.

6.2 Ground based OClO SCD offset correction method

For comparison with satellite observations, total slant column measurements must be obtained. This is achieved by selecting a fixed reference spectrum taken on a clear day when the station is not under the influence of chlorine-activated air masses. Usually the reference spectrum is updated each year to minimize biases due to possible instrumental instabilities. Residual offsets in the retrieved OClO SCDs may however be observed due to various possible reasons, such as (1) time-dependent instrumental effects leading to systematic spectral interference with OClO, (2) small residual OClO contamination of the selected reference spectrum, (3) spectral interference due to unknown atmospheric effects that may impact spectra and interfere with the OClO retrieval.

The offset correction applied in this study is based on the assumption that the offset source (if any) is constant during a twilight period. We have built a set of solar zenith angle dependent OClO AMFs, empirically obtained from observed OClO SCDs on a few sample activated days in late February and March in Harestua. These AMFs, which include photochemical effects, are then used to build daily AM and PM OClO Langley plots, from which offset values are derived and applied to original SCDs (see Figure 6.2 for an illustration). The underlying assumption is that the OClO amount in the fixed reference

spectrum is 0, and any offset found is therefore an artefact and should be removed. It must be noted that this approach is only applicable for observations covering a sufficiently large range of SZAs. The limit on the minimum solar zenith angle has been empirically set to 86°. For high latitude observations during polar night conditions, when the SZA constantly exceeds 86°, an estimate of the offset was obtained by fitting a polynomial function to offsets derived during the illuminated periods.

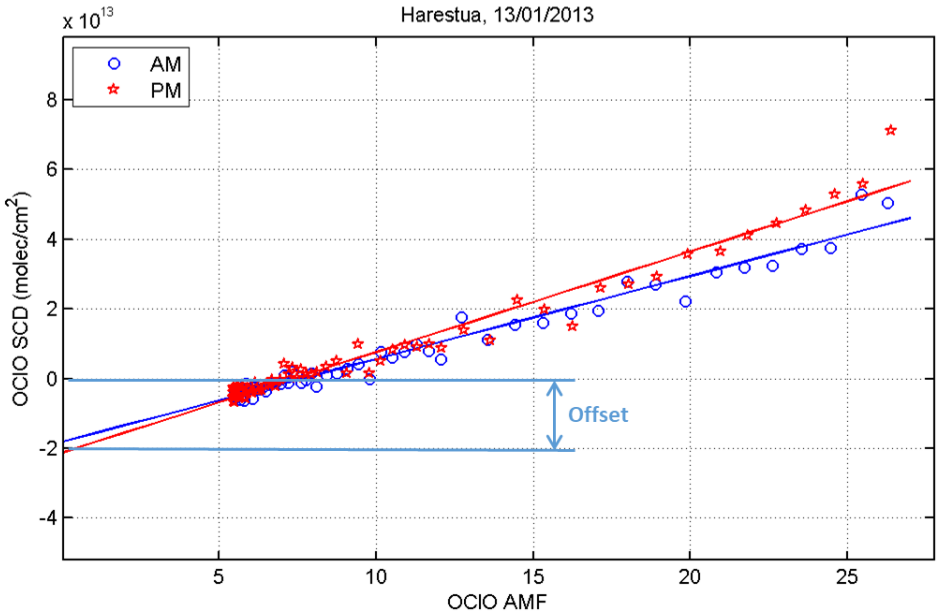

Figure 6.2: Illustration of an AM and PM OClO Langley plot for 13 January 2013 in Harestua.

This offset correction, which was derived independently for morning and evening data on each day, can be considered as objective as a) it is not linked to the satellite data and b) it is not based on subjective criteria such as the smoothness of the OClO time series.

7 Validation approach

The TROPOMI/S5p OClO validation approach adopted here follows the work done for the GOME-2/MetopA and -B validation within the AC SAF/EUMETSAT (Pinardi et al., 2017; Pinardi et al. 2022), and previous OClO validation studies (Richter et al., 2005; Oetjen et al., 2011). The comparison of OClO SCDs with ground-based SCD data relies on the assumption that satellite's AMF_nadir and ground-based AMF_zenith are similar. Oetjen et al. (2011) showed that AMFs from both geometries have similar values at large solar zenith angles. The AMF modelled for one day for Ny-Ålesund, based on the same model OClO vertical profile, agreed within 4% in the SZA range between 89° and 91° and by 13% at 80° SZA for the two observation geometries. The sensitivity of the AMF for the two geometries has been further investigated and is illustrated in Figure 7.1, confirming previous results.

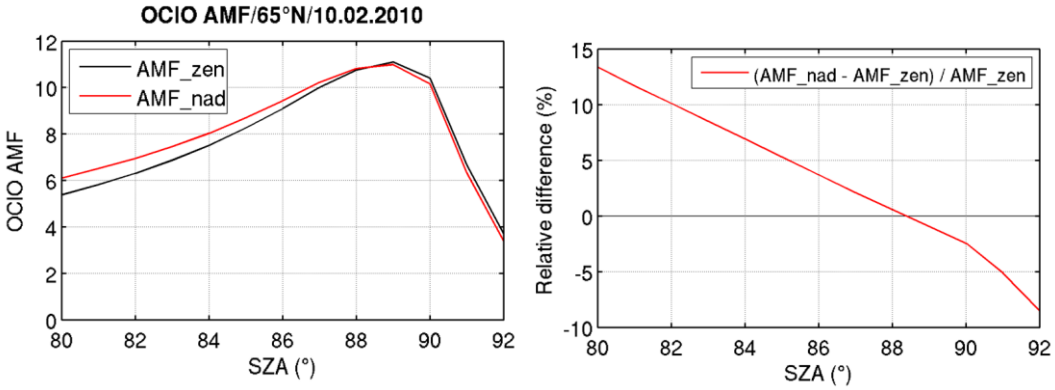

Figure 7.1: OClO AMF calculations for 65°N from ground-based zenith and satellite nadir geometries, from Pinardi et al., 2022.

All TROPOMI pixels within 200km radius around each ground-based station are selected for the overpasses. A daily average of these pixels is taken, in order to improve the signal-to-noise ratio, and the values are compared to the ground-based data. Coincidences are obtained by selecting ground-based data that are within ±1° SZA of the mean daily satellite value. Error weighted averages are performed using ground-based and satellite provided errors. In a future analysis, a selection per orbit could be tested, as well as some sensitivity study on different averaging in time and space (e.g. defined by the number of pixels and number of ground-based measurements).

7.1 Recommendations for data usage

In version v0.97 of S5p OClO, QA values are provided. Values of the QA value vary between 0 and 1, following criteria based on the quality of the fit, the SZA range and separation between ascending and descending parts of the orbit. The different meanings of the QA value are summarized in Table 7.1.

Globally, QA larger or equal than 0.5 are good OClO data with low RMS values, and large SZA are selected for QA>=0.7.

Table 7.1: Description of the different QA values meanings.

QA value	Meaning
0	Small SZA, High RMS, descending
0.1	Small SZA, High RMS, ascending
0.2	Large SZA, high RMS, descending
0.3	Large SZA, high RMS, ascending
0.5	Small SZA, low RMS, descending
0.6	Small SZA, low RMS, ascending
0.7	Large SZA, low RMS, descending
0.8	Large SZA, low RMS, ascending

Several tests with different QA selections have been performed for the validation, in addition to other possible filter selections (limitation of the S5p line-of-sight by limiting the viewing zenith angle) and impacts of changing some parameters of the comparison method. These are illustrated in Sect. 8.3.

8 Validation Results

8.1 Seasonal and short term variability

This section investigates if reference measurements and TROPOMI observations are able to capture similarly the short-term variability. Illustrations are grouped by hemisphere and comparisons are performed with the original ground-based data, as received from the data providers, and then after applying the ground-based offset correction introduced in Sect. 6.2.

8.1.1 Original ground-based data

Data of four stations have been collected for the validation of the TROPOMI columns around Antarctica. In this region, the OClO signal is stronger in the winter months, with values up to 5-10 x10^{14} molec/cm², when the stations are within the polar vortex. The vortex is created by the large-scale descent of cold air masses during winter, with the Coriolis force leading to strong circumpolar winds that prevent inner vortex air from mixing with out of vortex air. The polar vortex is one of the most important prerequisites for the chemical destruction of stratospheric ozone in this region. While the inhomogeneous distribution of landmasses in the Northern Hemisphere leads to frequent disturbances of the Arctic vortex by vertical propagation of planetary waves, the Antarctic vortex usually is more pronounced and persistent than the Arctic one.

The daily comparisons for the Antarctic are presented in Figure 8.1, separated per year. The 2018, 2019 and 2020 July-to-August periods all show an enhanced OClO signal (of 2-5x10^{14} molec/cm²), followed by a rapid decrease, and values close to zero from October to April.

The daily variations are sampled in a very coherent way from the ground and from space. Except for a clear negative bias in Belgrano and Neumayer October and November data and a positive bias in late 2018 in Marambio, the satellite and ground-based data agree very well in the enhanced OClO season, and reasonably well also for low levels of OClO. The biases in this last period are possibly due to a bad choice of the reference spectrum that was not completely free of OClO or due to instrumental instabilities not accounted for. The impact of these ground-based biases is tested later on in this section with ground-based data using the offset-correction introduced in Sect. 6.2.

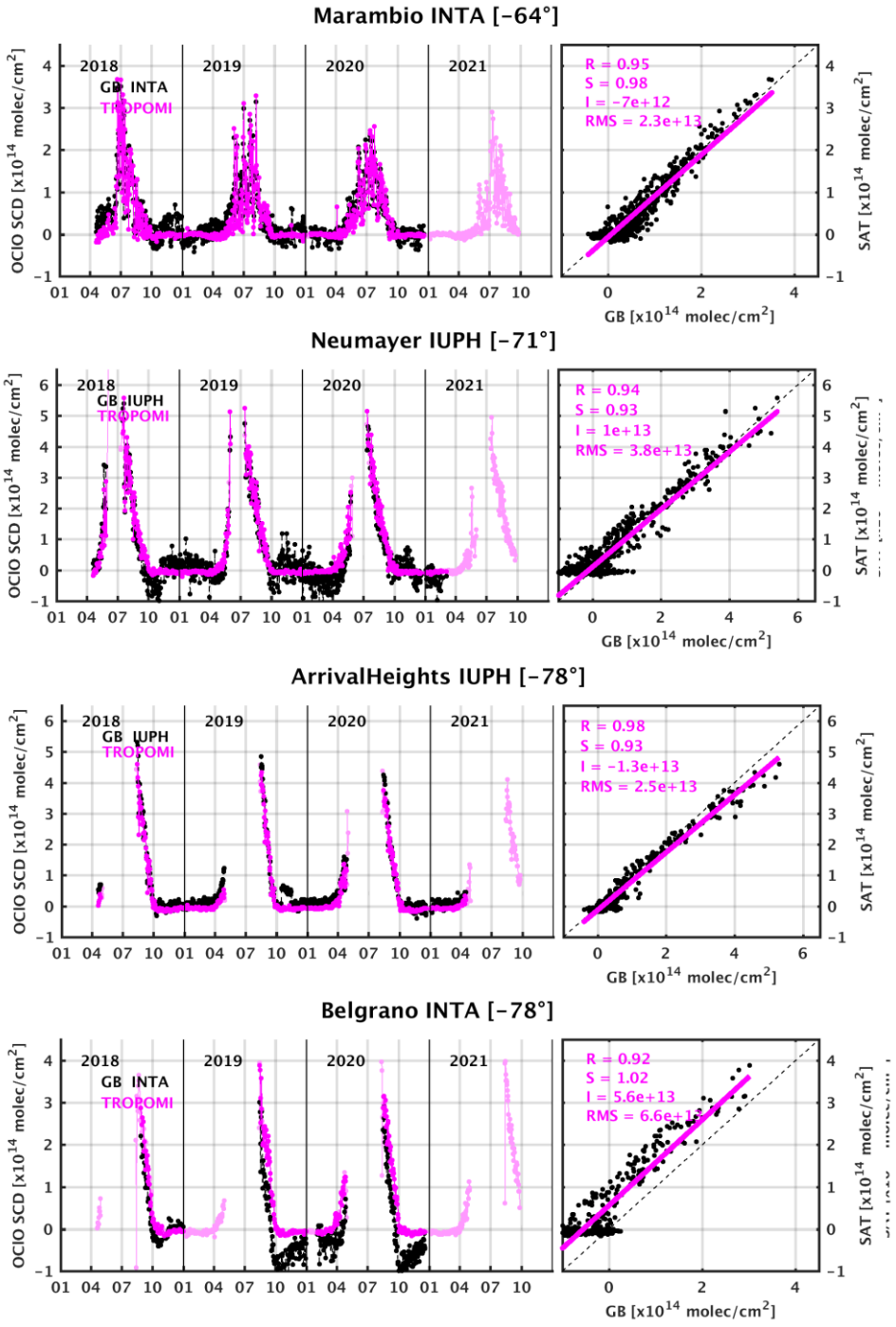

Figure 8.1: Time-series of TROPOMI and ground-based data over the Southern Hemisphere stations. Light pink are TROPOMI daily mean values, and the darker colors are the coincidences with the ground-based data. Scatter plots for each station are also included, with linear regression statistics.

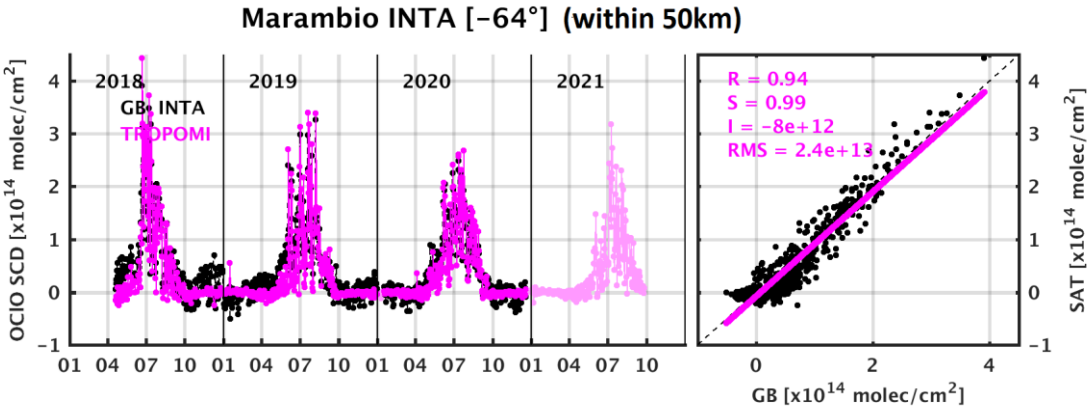

Figure 8.2: Time-series of coincident TROPOMI and Marambio ground-based data for selection of pixels within 50km around the station.

Day to day variability of several 1x10^{14} molec/cm² can be seen in Marambio during the activated period (June-July-August), and the saw tooth like behaviour indicates sampling of air-masses that are on the edge of the Antarctic polar vortex. The averaging of the satellite data within 200 km could mix air inside and outside the vortex, and thus a test with a selection of TROPOMI pixels within 50 km of Marambio station was done in order to try to reduce difference in vortex conditions, and presented in Figure 8.2. Small differences in the day-to-day time-series can be seen, but no big changes with respect to the baseline results of Figure 8.1.

Figure 8.3 presents the daily comparisons at the four stations distributed around the Arctic Circle: Eureka on the Queen Elizabeth Islands in northern Canada, Ny-Ålesund on Spitsbergen, Kiruna in Sweden and Harestua in Norway. Data are shown for the whole year, and OClO activation periods are expected from end of winter to spring, i.e. from December to April of each year. Kiruna and Harestua have S5p data for the whole period (light magenta dots), while for Ny-Ålesund and Eureka, the day-light only starts again around February-March. The OClO signals are highest in February 2020 at the highest latitude sites, and high peaks are seen over Kiruna in winter 2019/2020. In Harestua, the OClO signal is low for all the years, with values below 5 x10^{13} molec/cm², probably due to the polar vortex not extending as low as 60°N, except in winter 2020/2021 with values above 5 x10^{13} molec/cm² seen by both S5p and the ground-based instrument. At all stations, TROPOMI v0.97 and the zenith-sky DOAS instruments capture similarly the seasonal cycle of OClO, as well as day-to-day changes in OClO SCD. Differences from year to year and station to station exist, but typical enhanced OClO slant columns are found at the four sites in winter, with values up to 3x10^{14} molec/cm². However, as seen in Figure 8.1, also here several ground-based datasets present negative OClO columns in periods outside of the activated OClO period.

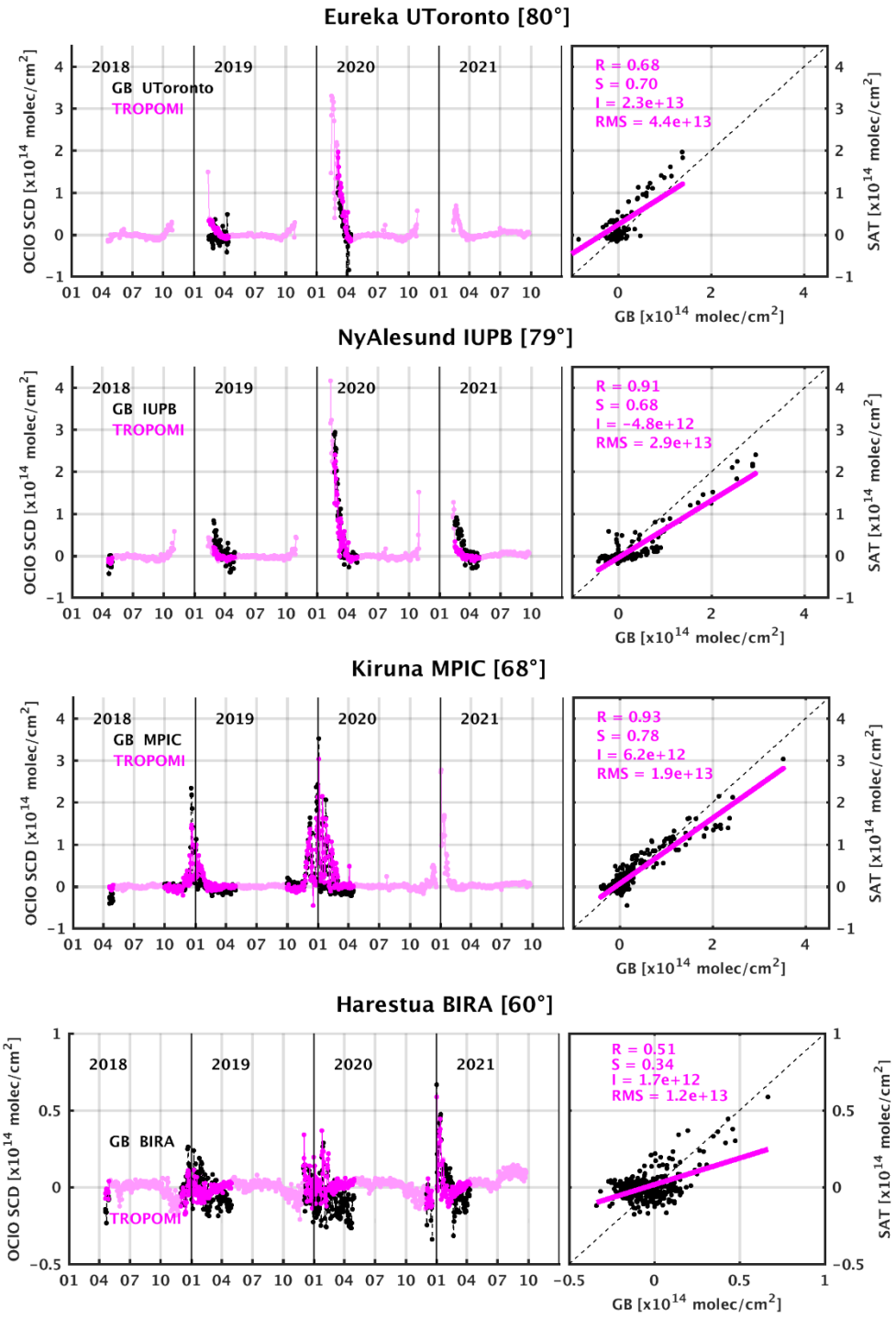

Figure 8.3: Time-series of TROPOMI and ground-based data over the Northern Hemisphere stations. Light pink are TROPOMI daily mean values, and the darker colors are the coincidences with the ground-based data. Scatter plots for each station are also included, with linear regression statistics. Note the different y-scale for Harestua.

8.1.2 Offset corrected ground-based data

As seen in Figure 8.1 and Figure 8.3, several ground-based datasets seem to be biased in low-OClO conditions. As discussed in Section 6.1, this could be due to not-optimal selection of the reference

spectra or instrumental instabilities and spectral interferences. In this section, the ground-based data were post-processed to estimate and correct for possible remaining biases, as discussed in Sect. 6.2. Figure 8.4 present the offset corrected comparisons for the Southern Hemisphere and Figure 8.5 for the Northern Hemisphere.

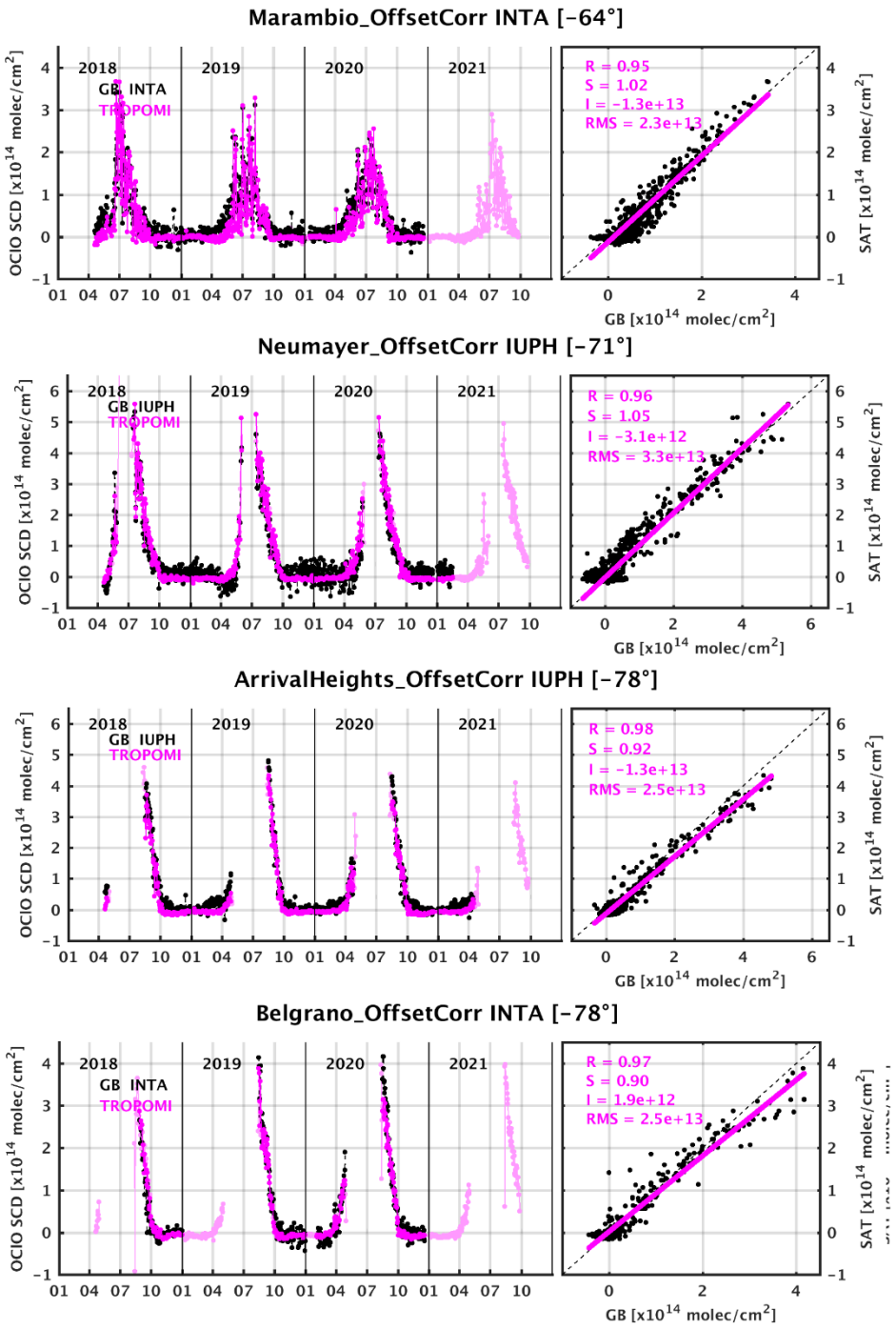

Figure 8.4: as Figure 8.1 but with the offset corrected ground-based datasets.

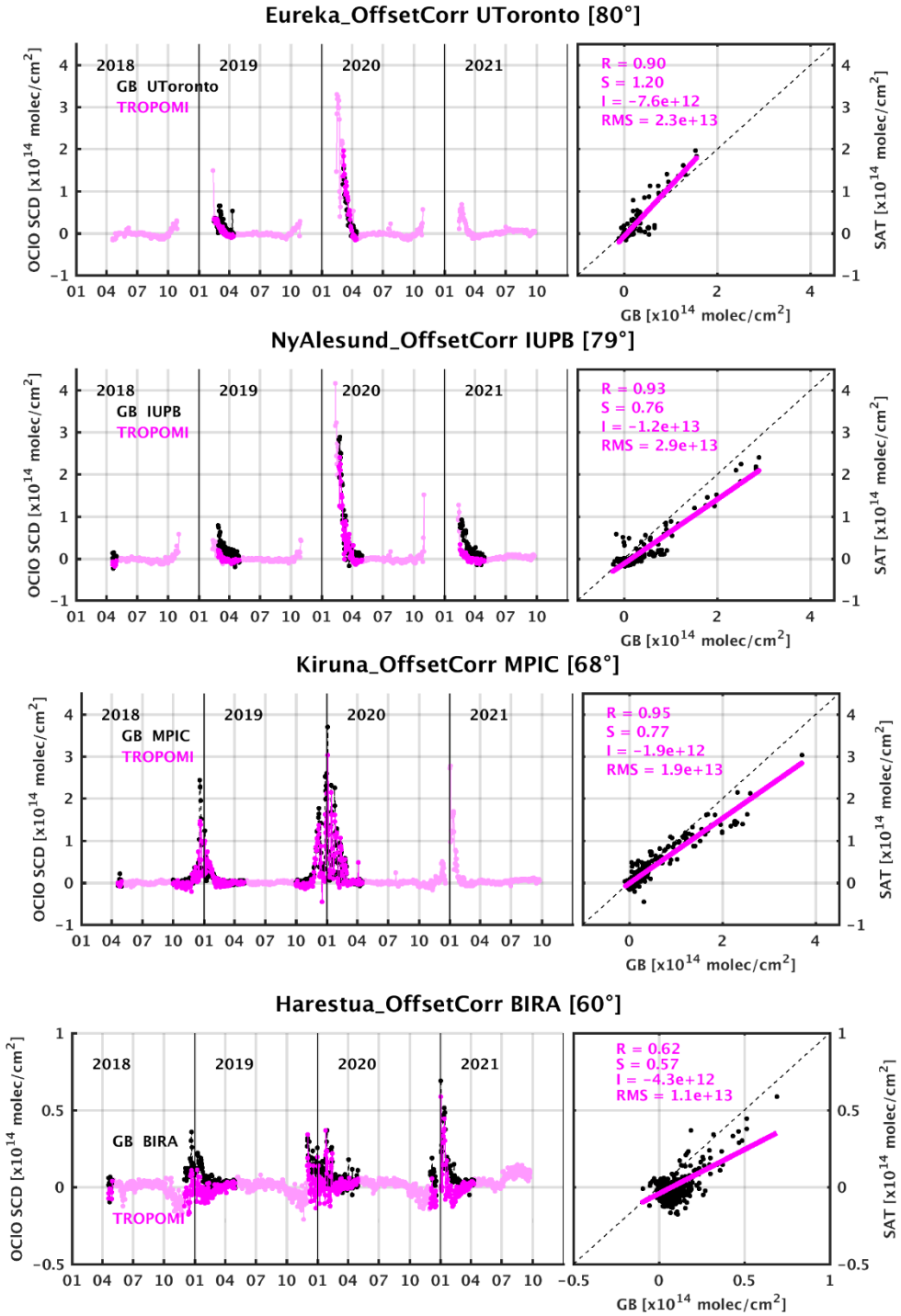

Figure 8.5: as Figure 8.3 but with the offset corrected ground-based datasets.

The clearest effect is for the stations in the Southern Hemisphere (Figure 8.4) that reported OClO SCD columns also in no-OClO periods. E.g., Arrival Heights negative data are shifted to around zero and Belgrano negative and slightly increasing data in October to December 2019 and 2020 are now flattened around zero. The effect is clear when looking at the statistical parameters of the linear regression: intercepts of about 1 and 5.6x10^{13} molec/cm² (Neumayer and Belgrano) are strongly reduced by (-0.3 and 0.2 x10^{13}), and changes in the slopes of about 10% are found.

Similarly, for the stations in the Northern Hemisphere, the offset correction is reducing the negative OClO SCD and the scatter around the zero values (e.g., Ny-Ålesund, Kiruna and Harestua) reducing the intercept and increasing the slopes and the correlation coefficients.

8.2 Scatter plots and absolute biases

The individual comparisons for Arctic and Antarctic stations after offset correction can be synthesized in order to have a "global" view of the quality of the TROPOMI v0.97 OClO SCD product. When considering all the stations together and focusing only on the activated period (July-August-September in the Southern Hemisphere and January-February-March in the Northern Hemisphere), scatter plots of satellite versus ground-based data can be drawn, as illustrated in Figure 8.6. The correlation coefficient is about 0.97, while the regression slope is 0.97 and the intercept is less than 0.2 $x10^{13}$ molec/cm². If we separate these results by hemisphere, the slopes are ~ 0.95/0.83, as seen in Figure 8.7, with a larger offset in the Southern Hemisphere and a lower slope in the Northern Hemisphere.

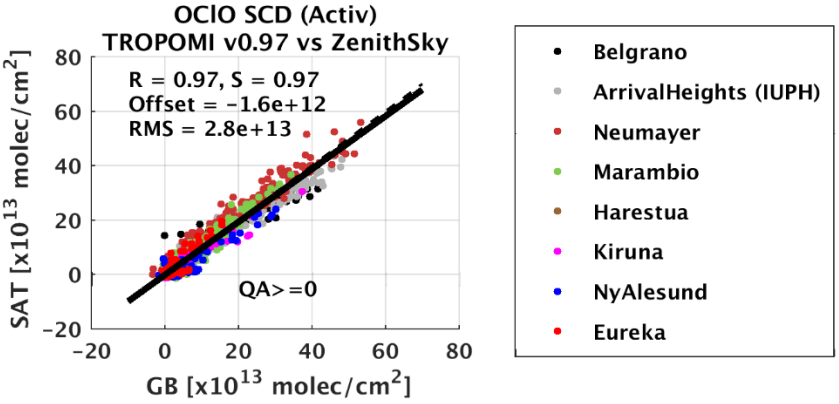

Figure 8.6: Scatter plot of TROPOMI and ground-based data over all stations, during activated months.

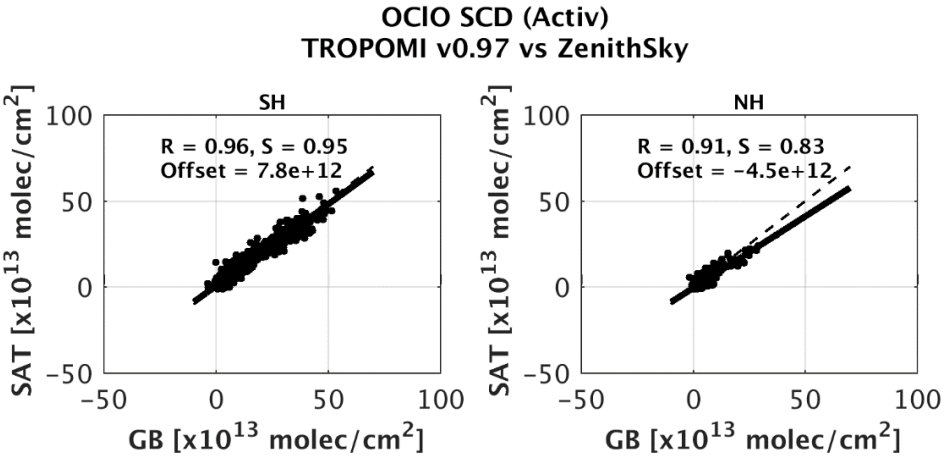

Figure 8.7: Scatter plot of TROPOMI and ground-based data over all stations, during activated months, separated per Hemisphere. Southern Hemisphere on the left panel, Northern Hemisphere on the right panel.

The overall validation results can also be summarized with an absolute satellite minus ground-based bias estimation at each station. Figure 8.8(left) presents the box-and-whisker plots of these differences for each station. The box plots correspond to the 25th and 75th percentile of the distribution, while the whiskers are the 9th and 91th percentile. On the right side, the corresponding scatter plot for all the stations together is also given. In the first line, the results with the baseline validation approach with all the pixels (QA>=0) described in Sect. 7, reported in black, are compared to when selecting only the good pixels (QA>=0.5). We can see that there is almost no impact on the daily mean comparisons for the polar stations, with only very few days rejected by this criteria (3 points, in Marambio).

The other lines of Figure 8.8 present the impact of the different QA filtering on the comparisons. QA>=0.5 is now used as a reference (black results) and testing QA=0.7 (large SZA, low RMS and descending part of the orbits only) strongly decrease the number of comparison points and degrade the comparison, reducing the sampling of OClO SCD from S5p to below 30x10^{13} molec/cm². The largest changes are in Neumayer and Marambio, leading to smaller correlation and slope and larger RMS. Testing QA=0.8 (only the ascending part of the orbits) only slightly degrades the comparisons, mostly in Neumayer and NyAlesund.

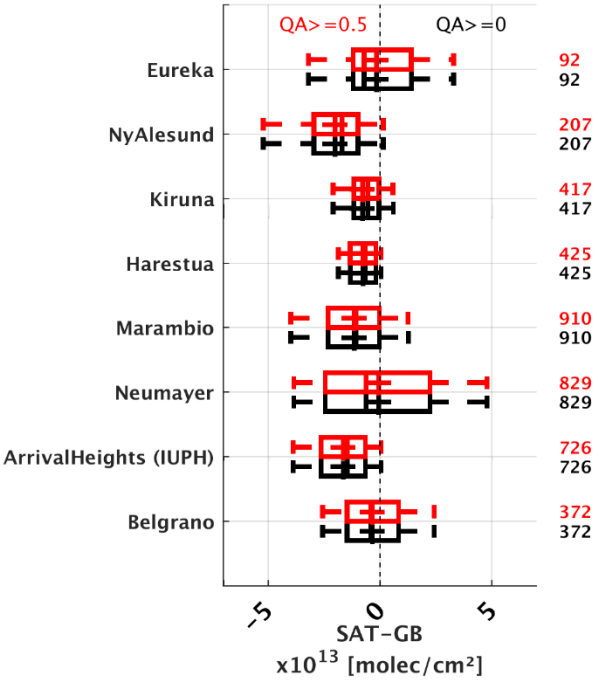

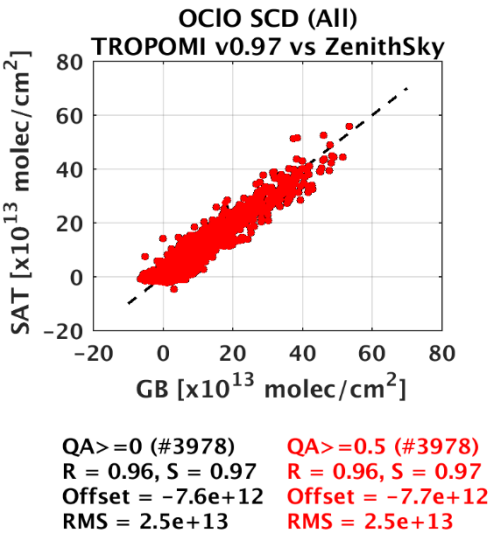

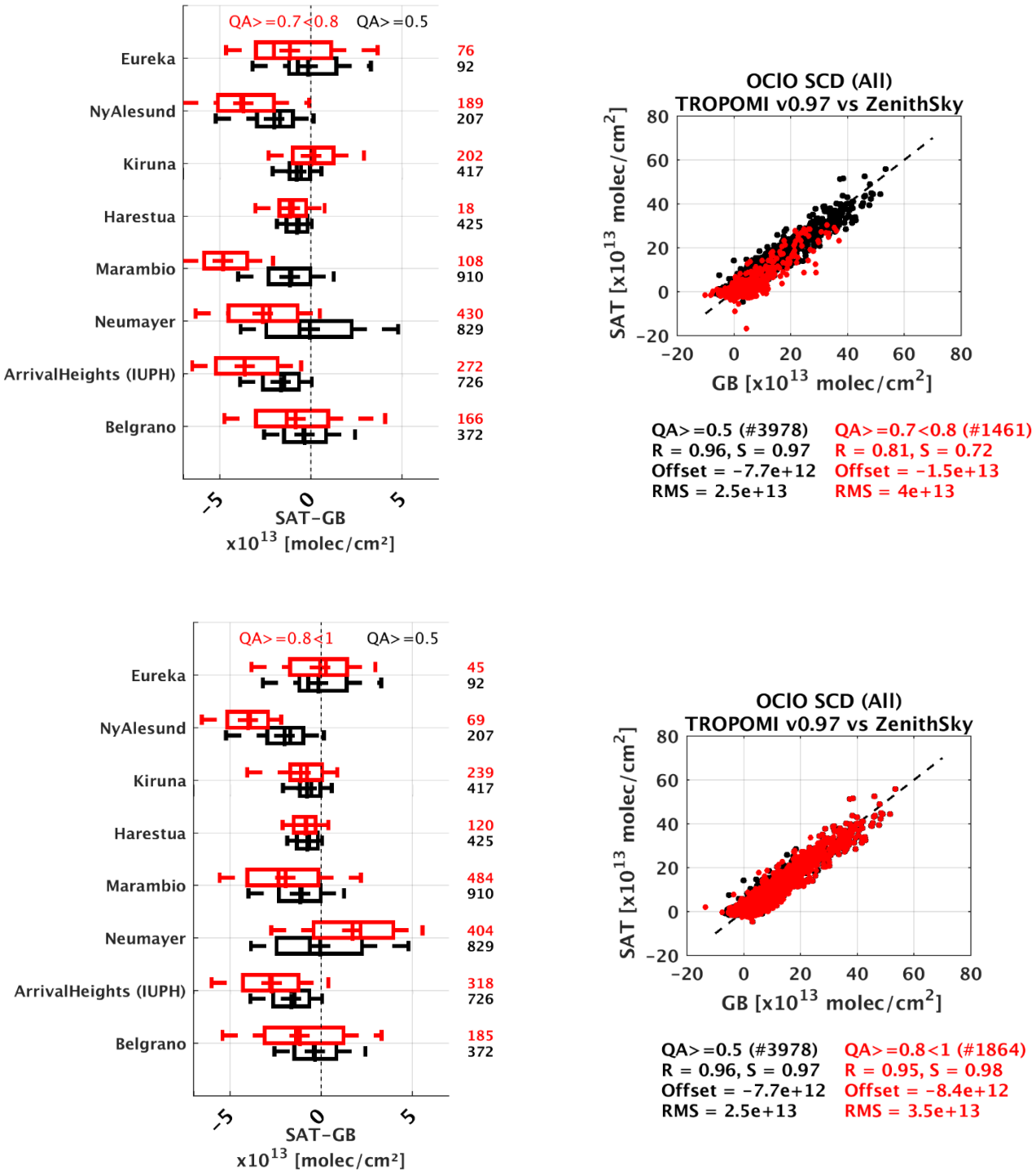

Figure 8.8: Overview of results with several QA filtering. (Left) Box and whisker plot of TROPOMI minus ground-based data over each station. (Right) Scatter plots of TROPOMI versus ground-based data for all stations.

Similarly, Figure 8.9 presents the results when: a) changing the colocation radius, b) only selecting activated periods, c) changing the way the daily average is done and d) limiting the S5p pixels to those having a small line-of-sight (absolute viewing zenith angle <30°).

Small variability in the results is found for the different tests, except for the Neumayer when selecting only the active months (July-August-September in this case). The median biases at each station are generally smaller than 1 x10^{13} molec/cm², with the largest value of 2.1 x10^{13} molec/cm² at Neumayer for the active period (compared to -6.2 x10^{12} molec/cm² over the whole period). The dispersion of the differences is generally larger than the median bias. Only small changes in the regression statistics are found for the different cases, with mostly an impact on the linear intercept value and the RMS.

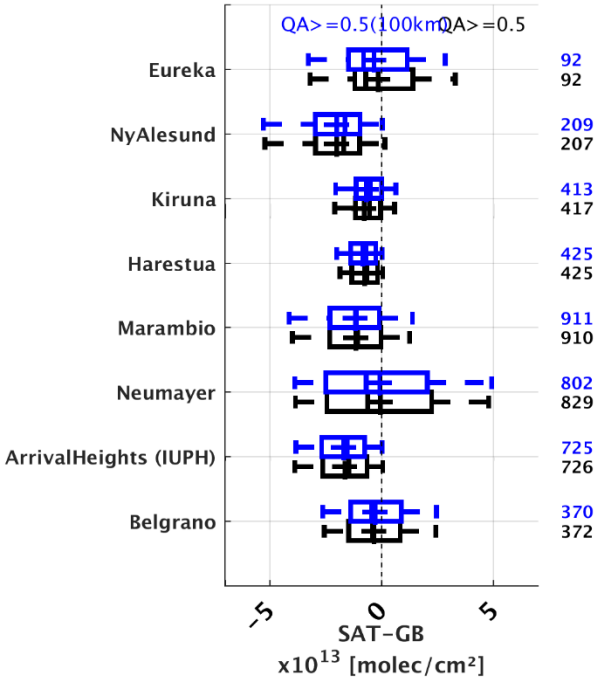

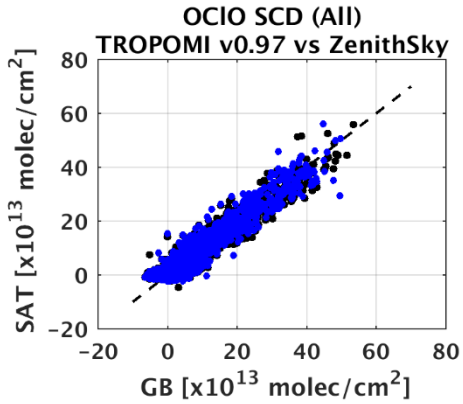

QA>=0.5 (#3978)
R = 0.96, S = 0.97
Offset = -7.7e+12
RMS = 2.5e+13

QA>=0.5(100km)
(#3947)
R = 0.95, S = 0.98
Offset = -8.3e+12
RMS = 2.5e+13

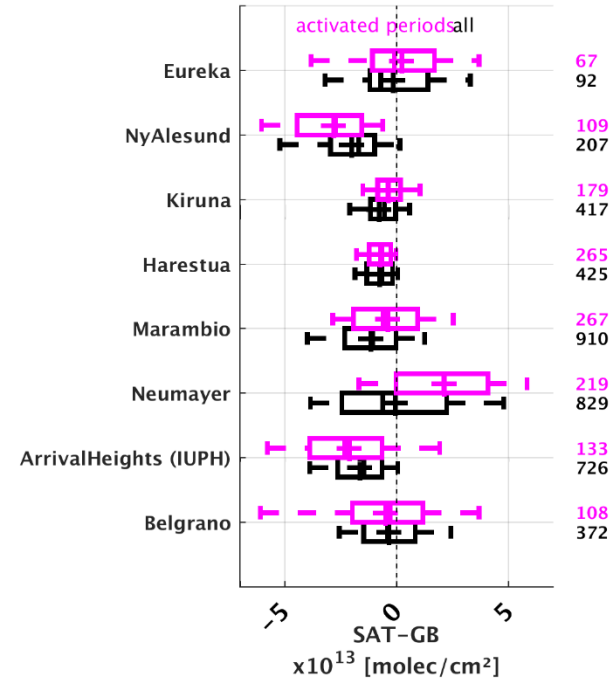

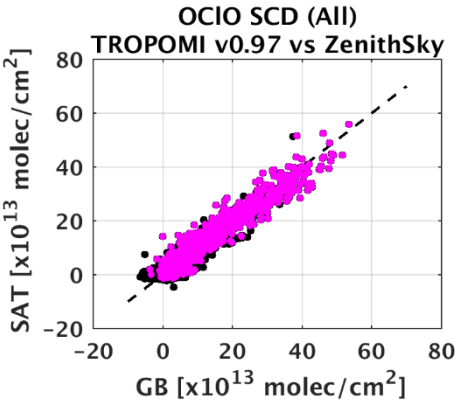

all (#3978)
R = 0.96, S = 0.97
Offset = -7.7e+12
RMS = 2.5e+13

activated periods
(#1347)
R = 0.97, S = 0.98
Offset = -1.8e+12
RMS = 2.8e+13

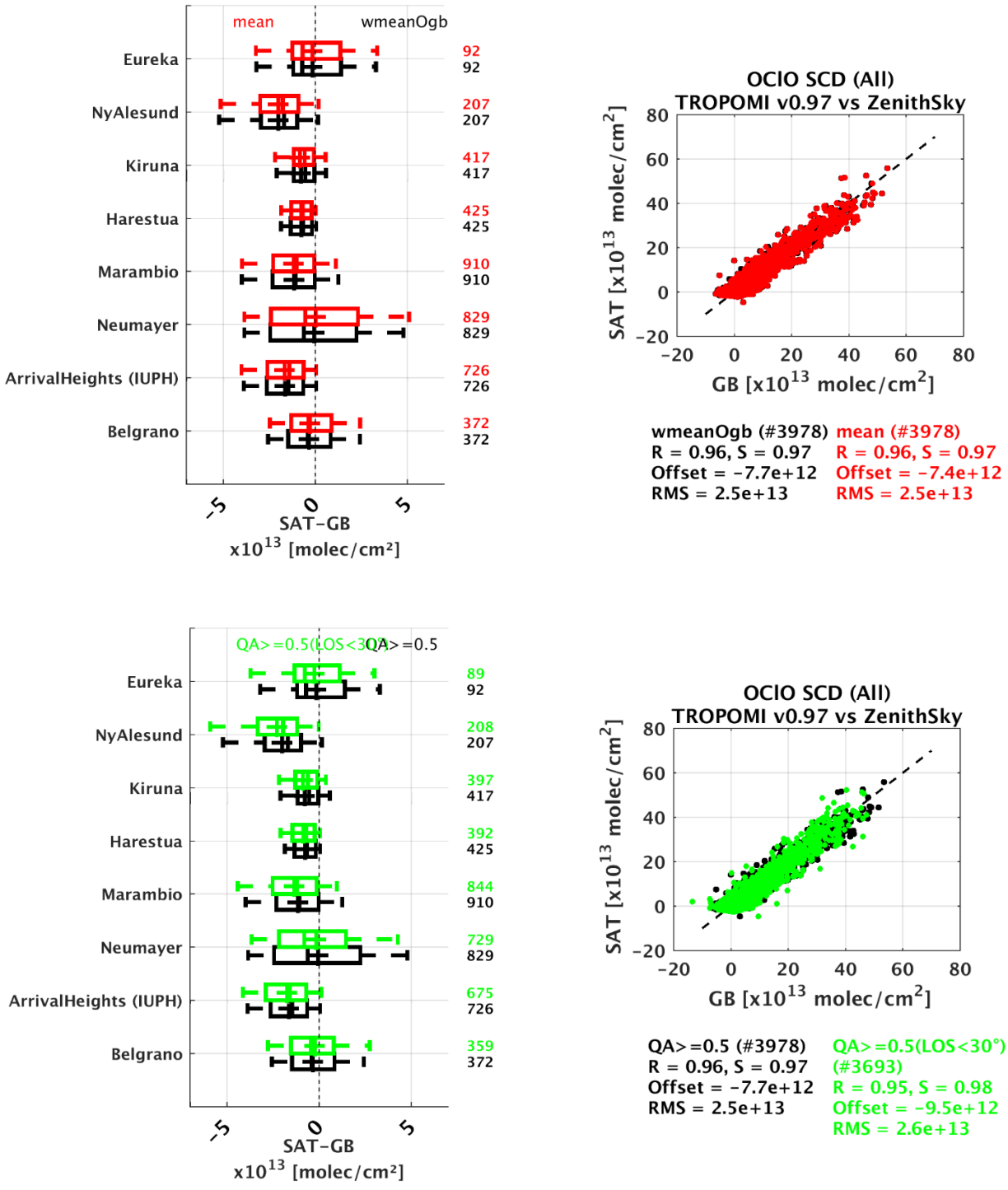

Figure 8.9: Box and whisker plot of TROPOMI minus ground-based data over each station. Several comparison settings are compared to the baseline comparison (black) that are done with QA>=0.5. (Blue) when taking a collocation radius of 100km instead of 200km; (magenta) when only considering the activated periods; (red) when doing an un-weighted average of the ground-based data ; (green) when filtering S5p for small line-of-sight (|viewing zenith angle|<30°).

Figure 8.10 presents, on the left, the comparison bias and its statistical error: Err = 2*MAD/sqrt(n), where MAD is the Median Absolute Deviation (MAD = k* median(abs(bias) - median(bias)), with k = 1.4826) and n is the number of comparisons. The bias is significant if it exceeds its statistical error (presented as grey bars), which is the case for almost all the sites here. On the right of Figure 8.9, the spread of the comparison (half the interpercentile 68) is compared to the TROPOMI estimated precision of about 2 x10^{13} molec/cm^2 (1σ estimation from the scatter in the equatorial Pacific, [AD4]). In all cases, except Neumayer, the spread is smaller than the estimated TROPOMI precision.

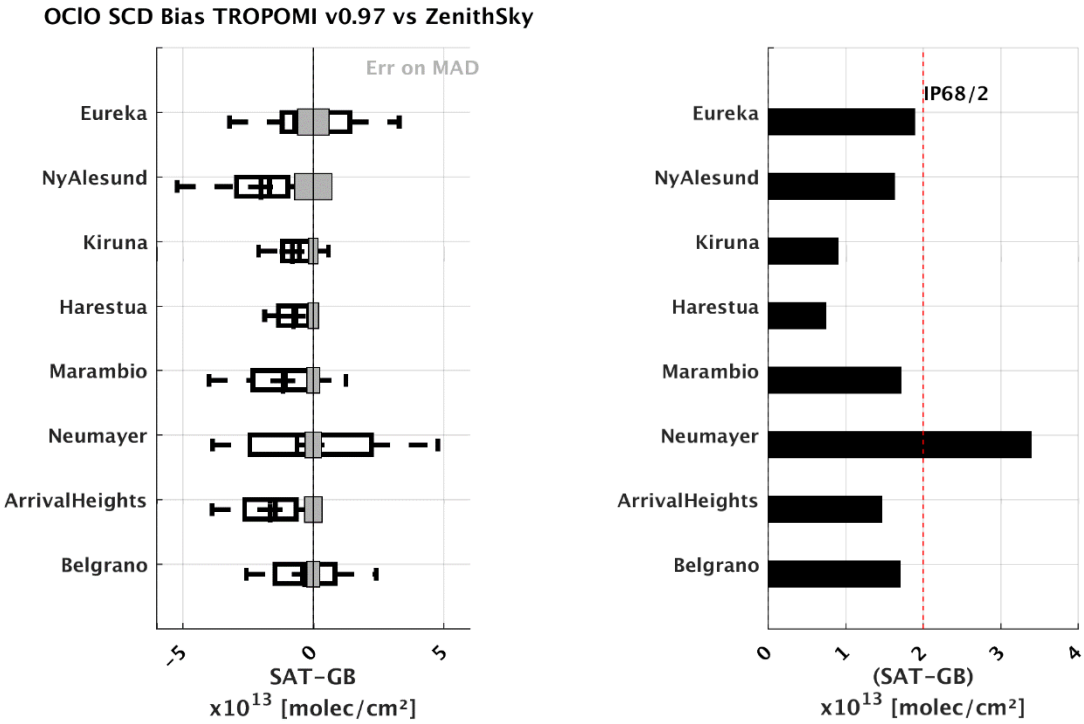

Figure 8.10: (left panel) Box and whisker plot of TROPOMI minus ground-based data and its statistical error (grey bars); (right panel) spread of the comparison and TROPOMI estimated precision of 2 x10^{13} molec/cm^2.

These results indicate that the largest part of the observed offsets is linked to uncertainties in the ground-based reference data and not the TROPOMI satellite product. However, after a correction of the ground-based offsets, considering all the stations together, such as in Figure 8.7, very good agreement is observed in both hemispheres (overall slopes of 0.95 and 0.83, with a larger intercept in the southern hemisphere of 0.8 x10^{13} molec/cm^2).

8.3 Dependence on influencing quantities

The dependence of the results as a function of a few influencing quantities has been evaluated. Figure 8.11 and Figure 8.12 show the results for the dependence on S5p SCD OClO magnitude and SZA, respectively.

It can be seen that the SAT-GB difference is generally larger than ±5 x10^{13} molec/cm² for SZA values above ~83° SZA (except for Neumayer where it is already the case for smaller SZA), and for TROPOMI

OClO SCD columns larger than 1x10^{14} molec/cm^2. This behavior could be at least partly explained by the averaging of satellite data over a 200 km radius, which smears out spatially confined maxima.

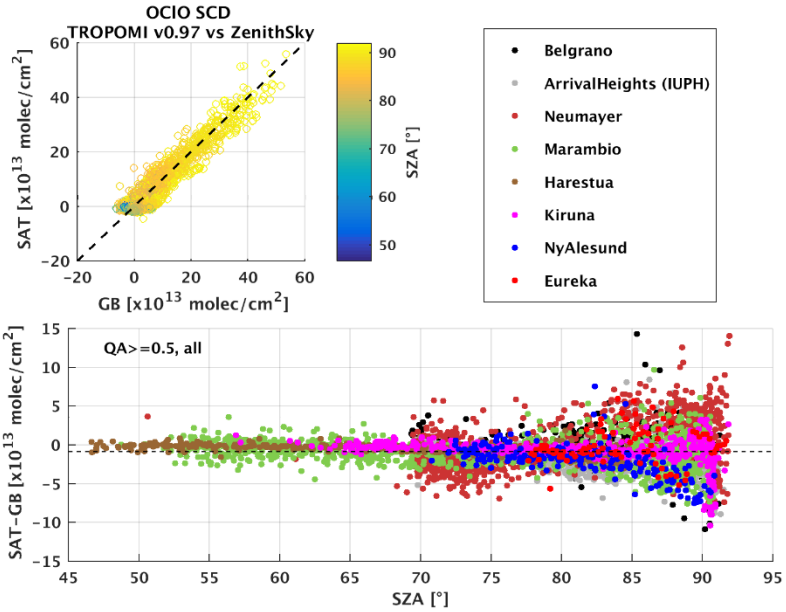

Figure 8.11: Scatter plot and absolute bias as a function of the Solar Zenith Angle, for the bias corrected ground-based sites.

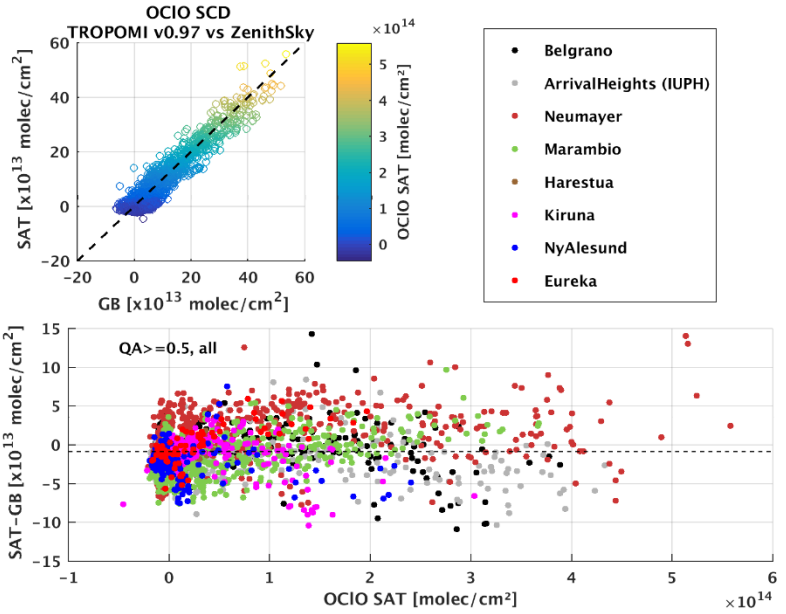

Figure 8.12: Scatter plot and absolute bias as a function of the TROPOMI OClO SCD, for the bias corrected ground-based sites.

9 Comparison to OMI satellite data

The OMI instrument has many similarities to the TROPOMI / S5p instrument – it is an imaging spectrometer with a similar spectral coverage and spectral resolution as S5p, and it is in a very similar early afternoon orbit. Therefore, OMI data are in principle a good source for comparison with S5p retrievals.

There is an operational OClO product from the Harvard Smithsonian Center available from NASA (https://disc.gsfc.nasa.gov/datasets/OMOCLO_003/summary). However, initial tests showed that for the period of S5p observations, this product does not provide meaningful values. The most probable reason is the degradation of the UV channel of the OMI instrument. To overcome this problem, a dedicated OMI OClO product was created at the University of Bremen based on the settings used for GOME-2A. While these data look good for the first years of OMI operation, they become noisy over time, and can only be used after averaging.

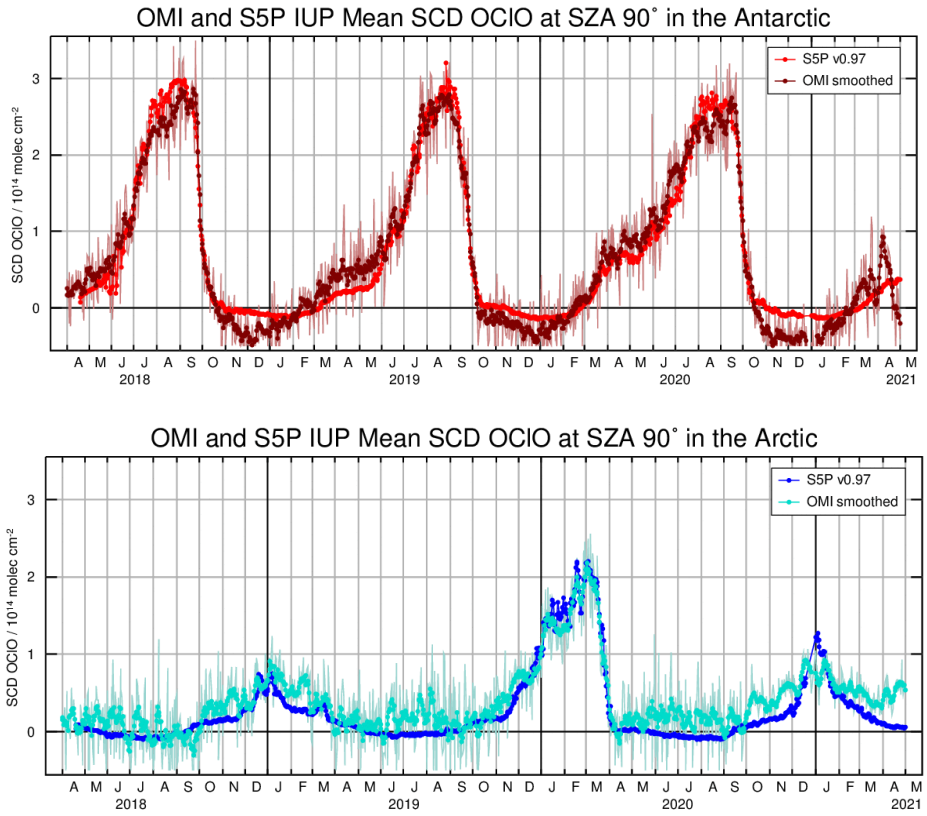

Figure 9.1: Comparison between OClO columns from S5p and OMI for the SH (top) and the NH (bottom). All data are sampled at 90° SZA. OMI data have been offset corrected and smoothed over 7 days for clarity (see text for details). The unsmoothed data are shown as thin line in the background.

As can be seen in Figure 9.1, there is overall good agreement between S5p and OMI OClO columns after offset correction. The offset is applied for each hemisphere separately and is 5×10^{13} molec/cm^2 for the Southern hemisphere and 12×10^{13} molec/cm^2 for the Northern Hemisphere. In the Southern Hemisphere, the agreement is very good with the exception of the time with no activation, where OMI data tend to be more negative than S5p data. In the Northern Hemisphere, OMI columns are larger

than S5p column with the exception of the strongly activated spring 2020. At the end of the time series, the agreement deteriorates in both hemispheres. The large scatter of the individual OMI retrievals highlights the excellent quality of the S5p data. It should however be kept in mind that OMI has already a life time of more than 15 years at the time of comparisons.

10 Comparison to GOME-2A satellite data

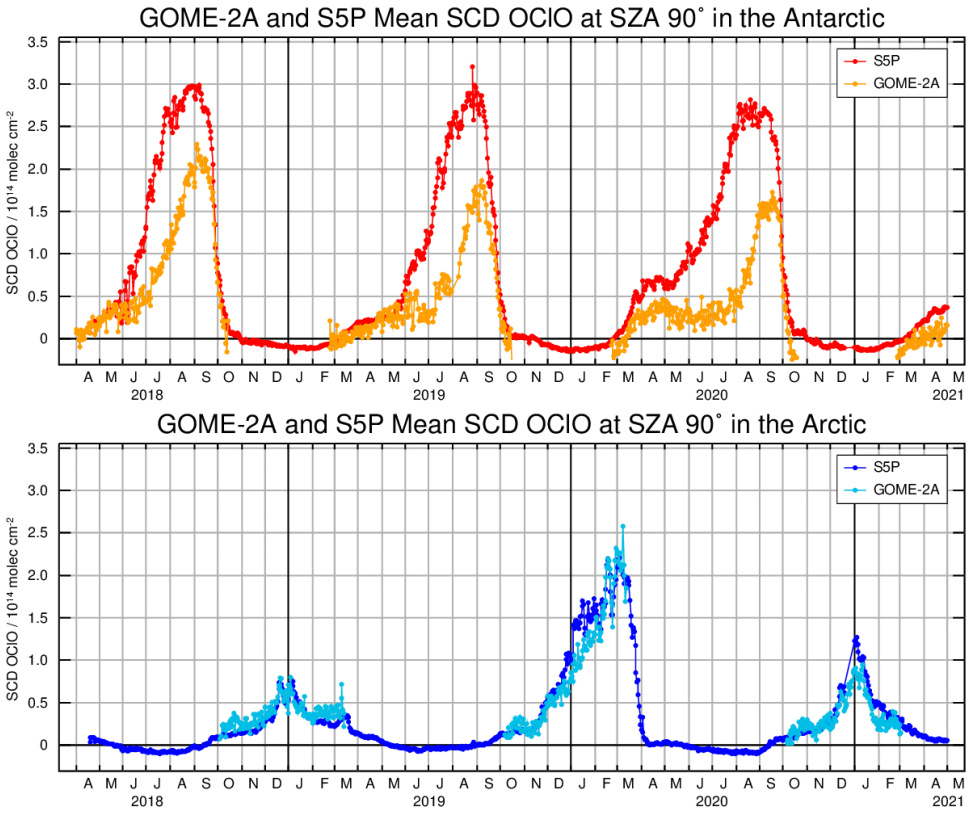

Figure 10.1: Comparison between OClO columns from S5p and from GOME-2A for the SH (top) and the NH (bottom). All data are sampled at 90° SZA, which corresponds to different latitudes for the two instruments. GOME-2A data have been offset corrected (see text for details).

A long and relatively stable OClO record exists from the GOME-2A instrument. This retrieval was developed in the context of two AC SAF (former O3M SAF) visiting scientist projects (Richter et al., 2009, 2015) and the data set extends from 2007 to the end of GOME-2A mission. In contrast to S5p data, the GOME-2A data set suffers from offsets, which change over time. Therefore, a two-step offset correction is applied before using the data: 1) the daily mean value over the equatorial region is subtracted and 2) an offset of 5×10^{13} molec/cm^2 is added to match the GOME-2A data to the S5p retrievals at the beginning of the activation period (March in the NH, October in the SH).

When comparing GOME-2A OClO columns with those of S5p, the different observational characteristics need to be taken into account. First, the local overpass time of GOME-2A is in the morning, while S5p is in an early afternoon orbit. As a result, the solar zenith angle at overpass is different for the two sensors, which is important for a photo-labile substance such as OClO. Thus, when evaluating data at 90° SZA, different latitudes are probed by the two instruments, potentially resulting

in different OClO columns if the sampling of the activated polar vortex is different in the two data sets. Second, the spatial coverage and resolution of GOME-2A is not as good as that of S5p, leading to differences in the area mapped, which again can have an impact on the observed OClO column. Finally, the orbit of GOME-2A was not maintained stable at the end of its mission, leading to a drift in local overpass time and thus sampled latitude.

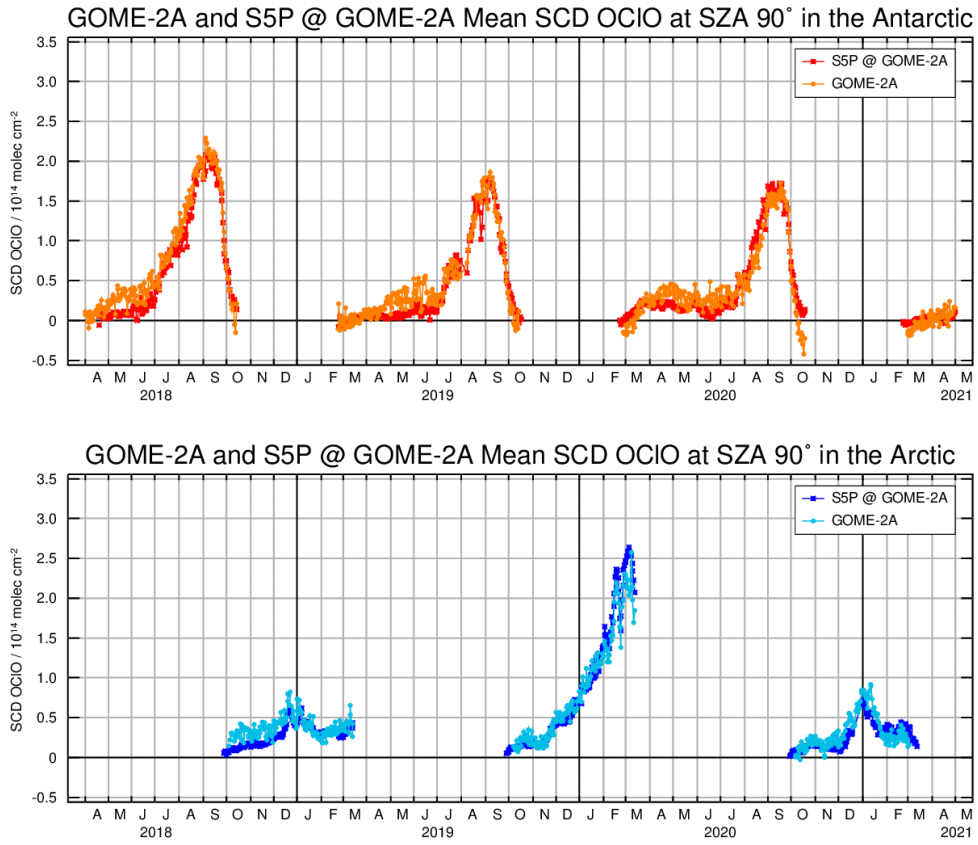

Figure 10.2: Comparison between OClO columns from S5p and from GOME-2A for the SH (top) and the NH (bottom). GOME-2A data are sampled at 90° SZA, while S5p data are sampled at the locations of the GOME-2A 90° SZA measurements. S5p data are thus not necessarily at 90° SZA.

As shown in Figure 10.1, direct comparison of GOME-2A and S5p OClO columns at 90° SZA show very good agreement in the NH but not in the SH. This is expected because of the time difference but needs to be taken into account when using the S5p data to extend the long-term GOME-2A record.

For a more meaningful comparison, the S5p data has been re-sampled at the locations of the GOME-2A measurements without applying a photochemical correction. The results are shown in Figure 10.2. In contrast to Figure 11.1, the agreement between the two data sets is now excellent in both hemispheres, indicating that the differences observed are mainly driven by the different sampling of the two instruments.

11 Comparison to MPIC S5p data

Independently of the Sentinel 5P innovation project, an alternative retrieval of OClO slant columns was developed at MPIC Mainz (Puķīte et al., 2021). This product is also based on TROPOMI radiances, but differs from the innovation project data in many aspects. The most important are

- Use of a radiance background at 60-65° SZA instead of the solar irradiance
- Inclusion of several additional fit parameters accounting for spectral effects like the temperature dependency of the Ring effect and Ring absorption effects and a higher-order term for the OClO SCD dependency on wavelength.
- Online determination of slit function.

The resulting product was already compared to the innovation product v0.96 in Puķīte et al., 2021, and excellent correlation was found. However, the slope of the regression line was around 1.1 with an offset of 4-5x10^{13} molec cm^{-2}, the innovation product being larger.

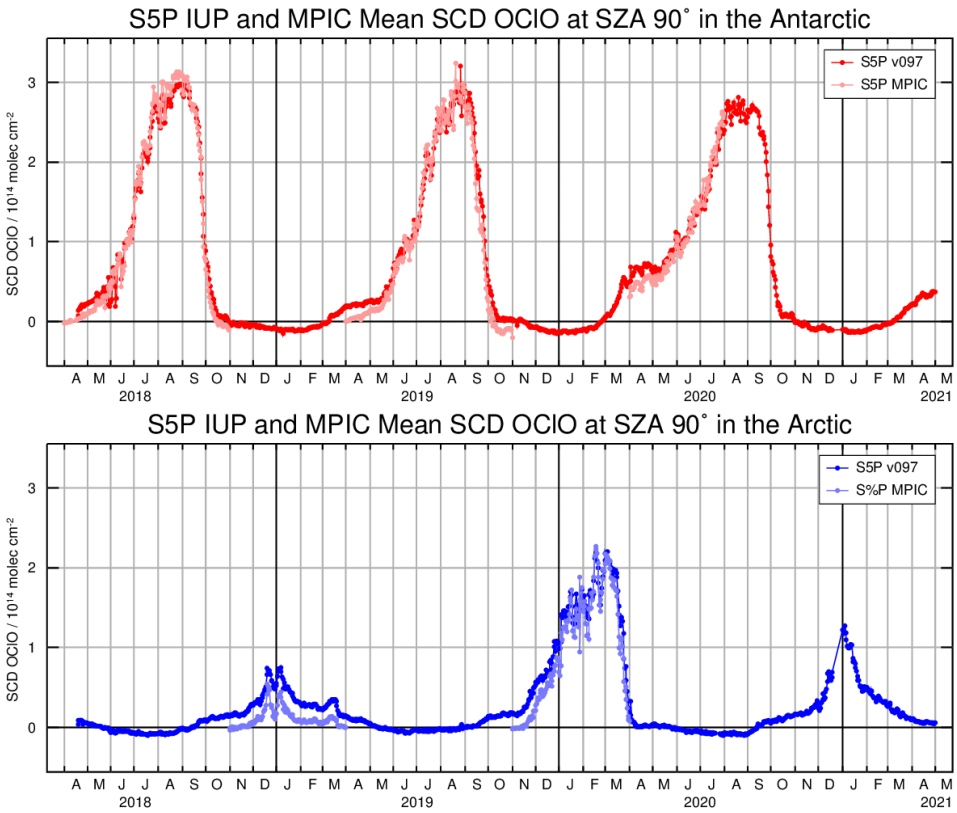

Figure 11.1: Comparison of the two S5p OClO products for the SH (top) and the NH (bottom). Data are sampled at 90° SZA.

Here, we repeat the comparison with v0.97 data. As shown in Figure 11.1, the agreement is excellent for the Southern Hemisphere and good for the Northern Hemisphere. Both absolute values and interannual variations are the same in the two products, as are the variations from day to day. The main difference are smaller values in the MPIC product outside the main activation period. The most probable reason for this mismatch is the use of a radiance background in the MPIC product, which will cancel any offsets in the data if they are also present at 65° SZA. It is difficult to decide which of the

two product is more realistic in these situations, but it cannot be excluded, that the offsets in the innovation product are the result of spectral interference and not the presence of OClO. The fact that similar offsets are found in OMI and GOME-2A data (see Sects. 9 and 10) indicates that this is either a real OClO background or a spectroscopic effect, but not an instrumental artefact.

12 Conclusions

This report investigated the quality of the S5p/TROPOMI OClO v0.97 slant columns datasets by comparing them to ground-based measurements and other satellite data sets.

For the validation, 8 DOAS zenith-sky stations around the Arctic and Antarctic regions were selected: Eureka (80°N), Ny-Ålesund (79°N), Kiruna (68°N), Harestua (60°N), Marambio (64°S), Belgrano (78°S), Neumayer (71°S) and Arrival Heights (78°S). OClO spectral analyses have been performed by each data provider individually using fixed noon spectra recorded at low SZA in the absence of chlorine activation. At each station, daily comparisons are performed by selecting satellite and ground-based SCD data pairs corresponding to similar SZA conditions, and by assuming that the AMF is similar for satellite and ground-based measurement in these geometries.

The following main conclusions can be drawn from the ground-based validation:

- Daily mean OClO SCD time-series show that satellite and ground-based observations agree well at all stations, both in terms of seasonal and inter-annual variabilities. Variations of the OClO column, from day-to-day fluctuations to the annual cycle, are captured consistently by both measurement systems.
- Several ground-based datasets seem to be biased (e.g. negative OClO SCD during periods where we do not expect OClO). An objective offset post-correction has been set up to correct for it in a harmonized way, which improves the comparisons with S5p in term of slopes, intercept and absolute bias.
- Results lead to correlation coefficient of about 0.97, slope of 0.97 and intercept of about -0.2×10^{13} molec/cm².

In terms of verification, comparisons have been performed against three other data sets: The MPIC retrieval for S5p, the OMI OClO product from University of Bremen and the GOME-2A OClO product from the University of Bremen. For all three data sets, time series of OClO columns at 90° SZA were compared. For the GOME-2A data which have a different overpass time, two versions for the S5p data were evaluated: the data taken at 90° SZA and the data sampled at the locations of the GOME-2A measurements.

The main conclusions from the satellite verification are:

- Excellent agreement is found with the MPIC product, the only difference being small variations in offset, presumably because of the use of a radiance background at 60-65° SZA in the MPIC data set.
- Agreement with OMI data is very good in absolute values and interannual variability, but both offsets and scatter are much larger in the OMI data, making quantitative comparison difficult.

- Agreement with GOME-2A data is good in the NH but not in the SH if both data sets are sampled independently at 90° SZA and thus at different latitudes. If S5p data is sampled to match the GOME-2A measurement pattern, agreement is very good for both hemispheres after correcting for GOME-2A offsets and drifts.

In summary, the S5p innovation OClO product performs very well compared to zenith-sky observations in both Polar Regions. The agreement with other satellite data is also very good, S5p clearly outperforming both OMI and GOME-2A in terms of noise, offsets and drift.

13 References

Bogumil, K., Orphal, J., Homann, T., Voigt, S., Spietz, P., Fleischmann, O.C., Vogel, A., Hartmann, M., Bovensmann, H., Frerik, J., and Burrows, J. P.: Measurements of molecular absorption spectra with the SCIAMACHY Pre-Flight Model: Instrument characterization and reference spectra for atmospheric remote sensing in the 230-2380 nm region, J. Photochem. Photobiol. A, 157, 167-184, 2003.

Fleischmann, O. C., et al.: New ultraviolet absorption cross-sections of BrO at atmospheric temperatures measured by time-windowing Fourier transform spectroscopy, J. Photochem. Photobiol. A, 168, 117–132, 2004.

Friess, U., Kreher, K., Johnston, P. V., and Platt, U.: Ground-based DOAS measurements of stratospheric trace gases at two Antarctic stations during the 2002 ozone hole period, J. Atmos. Sci., 62, 765–777, 2005.

Gil, M., Puentedura, O., Yela, M., Parrondo, C., Jadhav, D. B., and Thorkelsson, B.: OClO, NO2 and O3 total column observations over Iceland during the winter 1993/94, *Geophys. Res. Lett.*, **23**, 3337–3340, 1996.

Kreher, K., Keys, J. G., Johnston, P. V., Platt, U., and Liu, X.: Ground-based measurements of OClO and HCl in austral spring 1993 at Arrival Heights, Antarctica, *Geophys. Res. Lett.*, **23**, 1545–1548, 1996.

Kromminga, H., Orphal, J., Spietz, P., Voigt, S., and Burrows, J. P.: New measurements of OClO absorption cross-sections in the 325-435 nm region and their temperature dependence between 213 and 293 K, J. Photoch. Photobio. A, 157, 149–160, 2003.

Oetjen, H., Wittrock, F., Richter, A., Chipperfield, M. P., Medeke, T., Sheode, N., Sinnhuber, B.-M., Sinnhuber, M., and Burrows, J. P.: Evaluation of stratospheric chlorine chemistry for the Arctic spring 2005 using modelled and measured OClO column densities, *Atmos. Chem. Phys.*, **11**, 689-703, doi:10.5194/acp-11-689-2011, 2011.

Pinardi, G., Van Roozendael, M., Hendrick, F., Valks, P., : Validation report of GOME-2 GDP 4.8 OClO slant column data record for MetOp-A and -B DRR , AC SAF validation report, SAF/AC/IASB/VR/OClO, 29 May 2017 (https://acsaf.org/docs/vr /Validation_Report_DR_OClO_GDP48_May_2017.pdf

Pinardi, G., Van Roozendael, M., Hendrick, Richter, A., Valks, P., Bognar, K., Frieß, U., Granville, J., Gu, M., Johnston, P., Prados-Roman, C., Puentedura, O., Querel, R., Strong, K., Wagner, T., Wittrock, F. and

Yela Gonzalez, Y.: Ground-based validation of the MetopA and B GOME-2 OClO measurements, Atmos. Meas. Tech., 15, 3439–3463, https://doi.org/10.5194/amt-15-3439-2022 , 2022.

Puentedura, O., Yela, M., Navarro-Comas, M., Igleias, J., Ochoa, H., Halogen oxides from MAXDOAS observations at Belgrano II station (Antarctica, 78°S) in 2013, EGU poster 2014.

Puķīte, J., Borger, C., Dörner, S., Gu, M., Frieß, U., Meier, A. C., Enell, C.-F., Raffalski, U., Richter, A. and Wagner, T.: Retrieval algorithm for OClO from TROPOMI (TROPOspheric Monitoring Instrument) by differential optical absorption spectroscopy, Atmos. Meas. Tech., 14(12), 7595–7625, doi:10.5194/amt-14-7595-2021, 2021.

Richter A., Slijkhuis S., Loyola D., Offline Total OClO validation report, O3M-11, 2009. (http://www.iup.uni-bremen.de/doas/reports/o3saf_vs_gome-2_oclo_finalreport_091208.pdf)

Richter, A., M. Eisinger, A. Ladstätter-Weißenmayer and J. P. Burrows, DOAS zenith sky observations. 2. Seasonal variation of BrO over Bremen (53°N) 1994-1995, *J. Atm. Chem.*, **32**, 83-99, 1999.

Richter. A., Wittrock, F:, Valks, P., Evaluation of the possibility to derive reliable OClO slant columns from GOME2b and GOME2a spectra, O3M SAF VSA ID O3_AS14_02 final report, 2015 (http://www.iup.uni-bremen.de/doas/reports/o3m-saf_oclo_2_report_160427.pdf).

Rigby, M., Park, S., Saito, T., Western, L. M., Redington, A. L., Fang, X., Henne, S., Manning, A. J., Prinn, R. G., Dutton, G. S., Fraser, P. J., Ganesan, A. L., Hall, B. D., Harth, C. M., Kim, J., Kim, K. R., Krummel, P. B., Lee, T., Li, S., Liang, Q., Lunt, M. F., Montzka, S. A., Mühle, J., O'Doherty, S., Park, M. K., Reimann, S., Salameh, P. K., Simmonds, P., Tunnicliffe, R. L., Weiss, R. F., Yokouchi, Y. and Young, D.: Increase in CFC-11 emissions from eastern China based on atmospheric observations, Nature, 569(7757), 546–550, doi:10.1038/s41586-019-1193-4, 2019.

Serdyuchenko, A., Gorshelev, V., Weber, M., Chehade, W. and Burrows, J. P.: High spectral resolution ozone absorption cross-sections – Part 2: Temperature dependence, Atmos. Meas. Tech., 7(2), 625–636, doi:10.5194/amt-7-625-2014, 2014.

Solomon, S., Mount, G. H., Sanders, R. W., and Schmeltekopf, A. L.: Visible Spectroscopy at McMurdo Station, Antarctica – 2. Observations of OClO, J. Geophys. Res., 92, 8329–8338, 1987.

Solomon, S., Mount, G. H., Sanders, R. W., Jakoubek, R. O., and Schmeltekopf, A. L.: Observations of the nighttime abundance of OClO in the winter stratosphere above Thule, Greenland, *Science*, **242**, 550–555, 1988.

Tørnkvist, K. K., Arlander, D. W., and Sinnhuber, B. M.: Ground-based UV measurements of BrO and OClO over Ny-Ålesund during winter 1996 and 1997 and Andøya during winter 1998/1999, *J. Atmos. Chem.*, **43**, 75–106, 2002.

Vandaele, A. C., Hermans, C., Fally, S., Carleer, M., Colin, R., Mérienne, M. F., Jenouvrier, A. and Coquart, B.: High-resolution Fourier transform measurement of the NO2 visible and near-infrared absorption cross sections: Temperature and pressure effects, J. Geophys. Res. Atmos., 107(18), doi:10.1029/2001JD000971, 2002.

Vountas, M., Rozanov, V. V. and Burrows, J. P.: Ring effect: Impact of rotational Raman scattering on radiative transfer in Earth's atmosphere, J. Quant. Spectrosc. Radiat. Transf., 60(6), 943–961, doi:10.1016/S0022-4073(97)00186-6, 1998.

Wahner, A., G. S. Tyndall, and A. R. Ravishankara (1987), Absorption Cross-Sections for OClO as a Function of Temperature in the Wavelength Range 240-480 Nm, J Phys Chem-Us, 91(11), 2734-2738.

Wilmouth, D.M., Hanisco, T.F., Donahue, N.M., Anderson J.G. (1999), Fourier Transform Ultraviolet Spectroscopy of the $A^2\Pi_{3/2} \leftarrow X^2\Pi_{3/2}$ Transition of BrO, J. Phys. Chem, 103, doi:10.1021/jp991651o

Wittrock, F., Oetjen, H., Richter, A., Fietkau, S., Medeke, T., Rozanov, A., and Burrows, J.P. (2004), MAX-DOAS measurements of atmospheric trace gases in Ny-Ålesund – Radiative transfer studies and their application, Atmos. Chem. Phys., 4, 955–966, doi:10.5194/acp-4-955-2004.

Yela, M., C. Parrondo, M. Gil, S. Rodríguez, J. Araujo, H. Ochoa, G. Deferrari and S. Díaz, The September 2002 Antarctic vortex major warming as observed by visible spectroscopy and ozonesoundings. International Journal of Remote Sensing, V26, N16, 3361-3376, 2005.